

# A comparative analysis of spectral exponent estimation techniques for $1/f^\beta$ processes with applications to the analysis of stride interval time series

Alexander Schaefer<sup>a</sup>, Jennifer S. Brach<sup>b</sup>, Subashan Perera<sup>c</sup>, Ervin Sejdić<sup>a,\*</sup>

<sup>a</sup>*Department of Electrical and Computer Engineering, Swanson School of Engineering, University of Pittsburgh, Pittsburgh, PA, 15261, USA*

<sup>b</sup>*Department of Physical Therapy, University of Pittsburgh, Pittsburgh, PA, 15260, USA*

<sup>c</sup>*Department of Medicine, Division of Geriatrics, University of Pittsburgh, Pittsburgh, PA, 15261, USA*

---

## Abstract

**Background:** The time evolution and complex interactions of many nonlinear systems, such as in the human body, result in fractal types of parameter outcomes that exhibit self similarity over long time scales by a power law in the frequency spectrum  $S(f) = 1/f^\beta$ . The scaling exponent  $\beta$  is thus often interpreted as a “biomarker” of relative health and decline.

**New Method:** This paper presents a thorough comparative numerical analysis of fractal characterization techniques with specific consideration given to experimentally measured gait stride interval time series. The ideal fractal signals generated in the numerical analysis are constrained under varying lengths and biases indicative of a range of physiologically conceivable fractal signals. This analysis is to complement previous investigations of fractal characteristics in healthy and pathological gait stride interval time series, with which this study is compared.

**Results:** The results of our analysis showed that the averaged wavelet coef-

---

\*Corresponding author. E-mail: esejdic@ieee.org

ficient method consistently yielded the most accurate results.

Comparison with Existing Methods: Class dependent methods proved to be unsuitable for physiological time series. Detrended fluctuation analysis as most prevailing method in the literature exhibited large estimation variances.

Conclusions: The comparative numerical analysis and experimental applications provide a thorough basis for determining an appropriate and robust method for measuring and comparing a physiologically meaningful biomarker, the spectral index  $\beta$ . In consideration of the constraints of application, we note the significant drawbacks of detrended fluctuation analysis and conclude that the averaged wavelet coefficient method can provide reasonable consistency and accuracy for characterizing these fractal time series.

*Keywords:* fractals, time series analysis, self similarity, gait, stride intervals, detrended fluctuation analysis, wavelets, 1/f process

---

## 1 Introduction

The human body is comprised of many physiological systems which interact in a nonlinear manner (Eke et al., 2000, 2002; Glass, 2001; Glenny et al., 1991; Goldberger and West, 1987; Huikuri et al., 1998, 2000; Ivanov et al., 1999). Accordingly, changes in functional outcomes in a given physiological system may be caused by trends in either one or many other systems (Eke et al., 2000, 2002; Peng et al., 1995b). Disease, aging, genetic disorders, and trauma can have significant effects on many physiological functional outcomes like gait (Hausdorff et al., 1999, 2000, 1997, 1995, 1996). The locomotor system consists of a group of components from the central nervous, musculoskeletal, and other physiological systems. Generally, locomotor sys-

12 tem consists of the cerebellum, the motor cortex, and the basal ganglia,  
13 as well as visual, vestibular, and proprioceptive sensors (Hausdorff et al.,  
14 1995, 1996). This may be seen as a generalized control system. The cerebel-  
15 lum and basal ganglia receive information for processing, and sends control  
16 signals by the motor cortex. Current state information and feedback are  
17 provided by internal and external inputs from proprioceptive and sensory  
18 nerve and visual signals (Hausdorff et al., 1995, 1996; Eke et al., 2002). In  
19 a healthy subject, a stable walking pattern is maintained by the constant  
20 dynamic interaction between all of the components of the locomotor system.

21 Neurophysiological changes may alter the locomotor system's ability to  
22 correctly modulate dynamic changes in the gait process (Hausdorff et al.,  
23 1997). For example, decreased nerve conduction velocity, loss of motor neu-  
24 rons, decreased proprioception, muscle strength, and central processing ca-  
25 pabilities are notable declines due to advancing age (Hausdorff et al., 1997).  
26 Amyotrophic Lateral Sclerosis (ALS) is a neurodegenerative disease which  
27 severely affects the function of the motor neurons of the cerebral cortex,  
28 brain stem, and spinal cord (Hausdorff et al., 2000). Muscle weakness, in-  
29 creased fatigue and decreased endurance are characteristic of ALS (Sharma  
30 et al., 1995; Sharma and Miller, 1996). Parkinson's Disease (PD) and Hunt-  
31 ington's Disease (HD) are both neurodegenerative diseases which affect the  
32 basal ganglia (Hausdorff et al., 1997). PD and HD are marked by irregular  
33 of central motor control, the most apparent outcome of which is a chor-  
34 eiform or "dancing" like gait (Blin et al., 1990; Hausdorff et al., 1997). The  
35 common consequence among all of these disorders is increased stride inter-  
36 val time (Hausdorff et al., 1997). However, increased stride interval time  
37 alone is generally not indicative of any neurodegenerative disease, so the  
38 fluctuations of the stride interval must be considered to reveal any unique

39 mechanisms of decline (Hausdorff et al., 1997, 2000). It is apparent that in  
40 general, such changes to components of the locomotor system from disease  
41 and aging result in abnormal gait. However, the identity and severity of the  
42 underlying mechanism(s) causing the functional decline are still unknown,  
43 and can be extremely difficult to identify and characterize due to the highly  
44 nonlinear and complex interactions of the constituent physiological systems  
45 (Hausdorff et al., 1997, 2000; Bassingthwaighte, 1988; Bassingthwaighte and  
46 Bever, 1991).

47 Stride interval time series, like many physiological processes, have been  
48 observed to possess complex statistical properties (Glenny et al., 1991; Gold-  
49 berger and West, 1987; Ivanov et al., 1999; Hausdorff et al., 1997; Bassingth-  
50 waighte and Bever, 1991; Delignières et al., 2004; Kantelhardt et al., 2002;  
51 Peng et al., 1995a; Shlesinger, 1987). This phenomenon is due to the time  
52 evolution and complex interactions of many dynamical systems, imposed  
53 with random fluctuations, resulting in chaotic processes (Bak and Chen,  
54 1991). The goal of fractal time series analysis is to establish a metric which  
55 can indicate this property and the nature of the statistics, correlation, and  
56 other unique properties of time evolving system parameters (Delignières  
57 et al., 2004; Mandelbrot, 1985; Mandelbrot and Van Ness, 1968; Delignieres  
58 and Torre, 2009; Delignieres et al., 2006). The fractal description of pat-  
59 terns, self similarity, and statistical properties at many time scales can reveal  
60 new meaningful information about the process (Delignieres and Torre, 2009;  
61 Delignieres et al., 2006). Thus, these techniques are very useful when eval-  
62 uating physiological variables which are the outcome of complex dynamical  
63 system interaction.

64 The first primary aim of this paper is to clarify the interpretations of  
65 time series analyses for identifying the fractal properties of  $1/f^\beta$  type scale

66 invariant processes and highlight the inherent limitations of common meth-  
67 ods. To validate the concept of fractal time series analysis, a number of  
68 established time, frequency, and time-scale domain estimation techniques  
69 are implemented and tested. The tests include the entire range of  $1/f^\beta$  pro-  
70 cesses, with special consideration given to simulated signals most indicative  
71 of physiological processes. A matter which is often obfuscated in other stud-  
72 ies of fractal analysis was the choice of a metric for the fractal characteristic.  
73 For consistency, the process parameter  $\beta$ , also referred to as the spectral in-  
74 dex, was used as a metric for the fractal characteristic. The parameter  $\beta$  is  
75 convertible to other values commonly referred in the literature such as the  
76 fractal dimension  $D$ , the Hurst exponent  $H$ , and the scaling index  $\alpha$  (Eke  
77 et al., 2002).  $\beta$  was chosen for use here for its ease in interpretation with  
78 respect to the power law spectrum of  $1/f^\beta$  processes.

79 A second aim is to address the applications of these techniques to time  
80 series obtained in a physiological setting and their inherent constraints. A  
81 common limitation in acquiring physiological data, such as gait stride in-  
82 tervals, is the time series length (Eke et al., 2002; Delignieres et al., 2006;  
83 Bryce and Sprague, 2012). In many instances, the physical limitations of  
84 the test subject, equipment design, and other factors of the experimental  
85 setting limit the available length of acquired data. Accordingly, this pa-  
86 per will provide an evaluation of the algorithms with respect to short and  
87 long time series. It has also been recognized that the parameters of many  
88 physiological processes, such as stride interval time series, are by nature not  
89 zero mean (Hausdorff et al., 1999, 2000, 1997, 1995, 1996). To understand  
90 the effect of a time series with a nonzero mean, the estimation accuracy of  
91 each method was considered under three cases: (1) the normalized signal  
92 (2) the normalized signal with positive unit mean (3) a zero mean signal

93 from the normalized signal minus its mean. Finally, to verify the efficacy  
94 of the methods in the physiological setting, each method will be applied to  
95 published gait stride interval time series. The spectral index is calculated  
96 for gait time series from subjects with PD, HD, ALS and healthy controls  
97 (Hausdorff et al., 2000, 1996). The calculated values provide a comparative  
98 basis with respect to other studies aiming to determine long range correla-  
99 tions and fractal behavior of gait stride interval time series (Hausdorff et al.,  
100 1995; Delignieres and Torre, 2009).

## 101 **2. Power spectral densities of fractal process**

102 It has been noted that the power spectral density is an informative per-  
103 spective of fractal processes, which exhibits inverse power law scaling be-  
104 havior by  $S(f) = 1/f^\beta$ . Processes of this type are henceforth referred to  
105 as  $1/f^\beta$  processes (Eke et al., 2002; Delignieres and Torre, 2009; Shlesinger,  
106 1987; Kasdin, 1995; Chen et al., 1997; Pilgram and Kaplan, 1998). Generally  
107  $1/f^\beta$  process can be classified as belonging to one of two classes, fractional  
108 Gaussian noise (fGn) or fractional Brownian motion (fBm) (Eke et al., 2002;  
109 Delignieres et al., 2006). For fGn class signals, the probability distribution  
110 of a segment of the signal is independent of the segment size and its tempo-  
111 ral position in the signal (Eke et al., 2002). Thus, the correlation structure  
112 and any statistical descriptions of the process do not change over time, so  
113 the process is stationary (Delignieres and Torre, 2009). In an fBm signal,  
114 the probability distribution in a larger segment is equal to a distribution  
115 in a smaller segment when the distribution in the large segment is rescaled  
116 (Eke et al., 2002). Here, the inverse power law relationship is observed for

117 the calculation of some statistical measure  $m$  on the segment of length  $n$

$$\log m_n = \log p + H \log n \quad (1)$$

118 This implies the power law relationship where  $p$  is a proportionality factor  
119 and  $H$  is the Hurst exponent and  $H \in [0, 1]$ . The Hurst exponent is a com-  
120 monly used metric for indicating the fractal nature of a fractional Gaussian  
121 noise or fractional Brownian motion process (Cannon et al., 1997; Davies  
122 and Harte, 1987; Crevecoeur et al., 2010). These processes have the prop-  
123 erty that the cumulative summation of an fGn signal results in a fBm signal  
124 (Eke et al., 2002). As a result, a given process is interconvertible from one  
125 class to the other by the integral or derivative (Eke et al., 2002; Shlesinger,  
126 1987; Kasdin, 1995; Chen et al., 1997; Pilgram and Kaplan, 1998). This ne-  
127 cessitates a unique Hurst exponent specific to each class of processes. These  
128 can be denoted  $H_{fGn} \in [0, 1]$  and  $H_{fBm} \in [0, 1]$  (Eke et al., 2002; Delignieres  
129 et al., 2006).  $H = 0.5$  in each class is the special case, where  $H_{fGn} = 0.5$  is  
130 white Gaussian noise ( $\beta = 0$ ) and  $H_{fBm} = 0.5$  is Brownian motion ( $\beta = 2$ )  
131 (Eke et al., 2002; Delignieres and Torre, 2009). White Gaussian noise is  
132 the characteristic process of the fractional Gaussian noise class of  $1/f^\beta$  pro-  
133 cesses (Eke et al., 2002). The important property of white Gaussian noise  
134 is that energy is equally distributed for all frequencies. Thus, it has a flat  
135 power spectrum and  $\beta = 0$ .  $H_{fGn} < 0.5$  is anti-correlated Gaussian noise,  
136 and  $H_{fGn} > 0.5$  is correlated noise (Delignieres and Torre, 2009). Brownian  
137 motion is the characteristic process for the fBm class. These processes ex-  
138 hibit a  $1/f^\beta$  power spectrum where  $\beta = 2$  (Eke et al., 2002; Hausdorff et al.,  
139 2000). In this case, successive outcomes in the process are correlated, and  
140 the process exhibits non-stationary time evolution (Delignieres and Torre,  
141 2009).  $H_{fBm} < 0.5$  is anti-persistent Brownian motion, and  $H_{fBm} > 0.5$

142 is persistent Brownian motion, where  $H_{fBm} = 0$  is pink noise of  $1/f^1$  (Eke  
 143 et al., 2002). Shown in Figure 1 (a) (c) and (e) are fGn signals of  $H = 0$ ,  
 144 0.5, 1 and their corresponding (cumulatively summed) fBm signals Figure 1  
 145 (b) (d) and (f). This provides an overview of signals of each process class  
 146 and their interconvertible relationship.

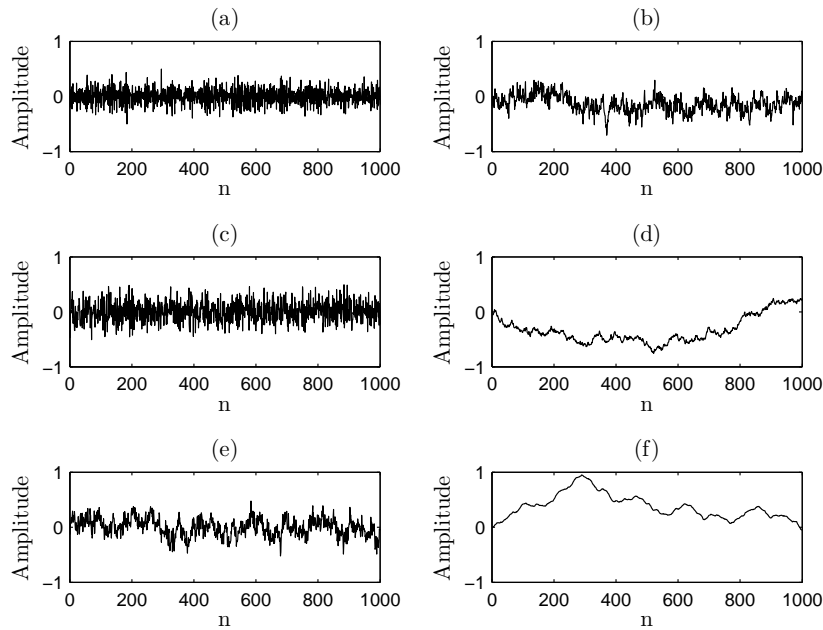


Figure 1: Range of fGn and fBm class signals: (a)  $H_{fGn} = 0$ ; (b)  
 $H_{fBm} = 0$ ; (c)  $H_{fGn} = 0.5$ ; (d)  $H_{fBm} = 0.5$ ; (e)  $H_{fGn} = 1$ ; and (f)  
 $H_{fBm} = 1$ .

147 In the case where  $\beta = 1$ , some correlation between timescales exists  
 148 but is weak (Delignieres et al., 2006). In summary, a given process can be  
 149 classified as belonging to one of these two distinct classes where  $\beta = 1$  is the  
 150 distinct boundary between each (Kasdin, 1995). The relationship between



151 each class's Hurst exponent and the power spectrum  $1/f^\beta$  can be observed  
152 by the by the following relationships (Eke et al., 2002)

$$H_{fGn} = \frac{\beta + 1}{2} \quad (2)$$

153

$$H_{fBm} = \frac{\beta - 1}{2} \quad (3)$$

154 Thus, the range of all fGn and fBm processes for  $0 < H < 1$  correspond  
155 to  $-1 < \beta < 3$ , where the boundary between each class lies at  $\beta = 1$   
156 (Eke et al., 2002; Delignieres et al., 2006). Figure 2 gives an overview of an  
157 fGn Gaussian white noise ( $\beta = 0$ ), pink noise ( $\beta = 1$ ), and fBm Brownian  
158 motion or red noise ( $\beta = 2$ ). Adjacent to each signal is its its log-log power  
159 spectrum, and the linear regression with slope indicating the corresponding  
160  $\beta$  value.

161 Many well developed fractal estimation algorithms for finding the Hurst  
162 exponent are specific to each process class. The choice of a method to evalu-  
163 ate the fractal properties of a signal will accordingly be difficult in a setting  
164 where it is unclear which of the two classes the signal belongs. If such  
165 methods are inappropriately applied, the calculated class specific Hurst ex-  
166 ponent will be incorrect. Consequently, its interpretation as a physiological  
167 biomarker will be ambiguous and potentially misleading. Awareness of this  
168 hazard is especially critical whenever the process lies at the boundary be-  
169 tween fractional Gaussian noise and fractional Brownian motion. This case,  
170 when  $\beta = 1$ , a signal represents the type of fractal process most typically  
171 exhibited by physiological systems (Eke et al., 2002; Glass, 2001; Goldberger  
172 and West, 1987; Huikuri et al., 1998, 2000; Ivanov et al., 1999; Peng et al.,  
173 1995a; Sejdić and Lipsitz, 2013). As a result of this dichotomy, signal clas-  
174 sification, the choice of a fractal characterization method, and the interpre-  
175 tation of its result becomes a critical yet inherently difficult procedure.

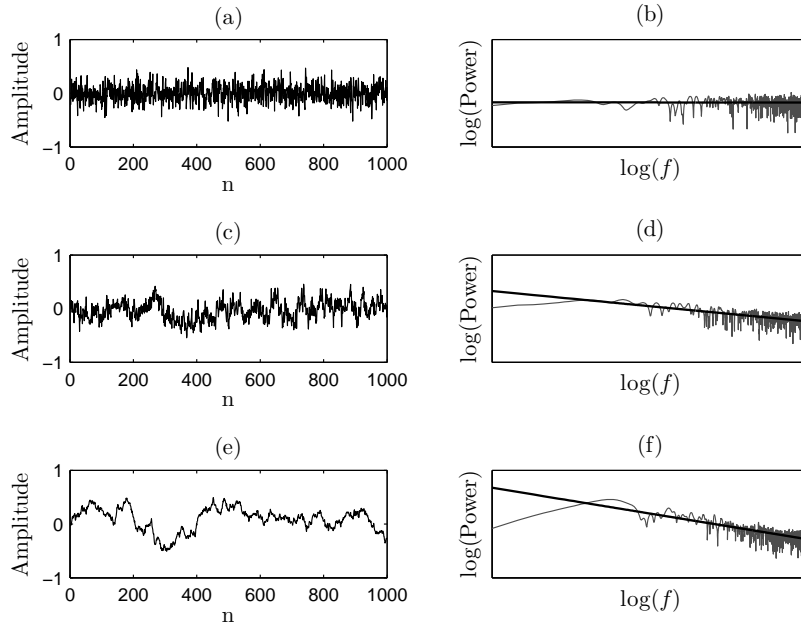


Figure 2: Sample time series and corresponding PSD with regression: (a) time series for  $\beta = 0$ ; (b) PSD of  $\beta = 0$  time series; (c) time series for  $\beta = 1$ ; (d) PSD of  $\beta = 1$  time series; (e) time series for  $\beta = 1$ ; and (f) PSD of  $\beta = 2$  time series.

### 176 3. Algorithms for estimation of $\beta$ values

177 For a  $1/f^\beta$  process,  $\beta$  values can be estimated in time, frequency or time-  
 178 frequency (time-scale) domains. Here, we overview several most prominent  
 179 implementations in literature concerned with characterizing physiological  
 180 phenomena.

181 *3.1. Time Domain*

182 This section overviews the three time domain fractal techniques imple-  
183 mented here. These are dispersional analysis, bridge detrended scaled win-  
184 dow variance (bdSWV), and detrended fluctuation analysis (DFA).

185 *3.1.1. Dispersional Analysis*

186 For dispersional analysis, we refer to the proposal of this technique  
187 by Bassingthwaighte, et al (Bassingthwaighte, 1988; Bassingthwaighte and  
188 Bever, 1991; Bassingthwaighte and Raymond, 1995, 1994). This time do-  
189 main based algorithm estimates the fractal characteristic by the variances  
190 of the mean of signal segments. Then, the standard deviation on various  
191 intervals is plotted versus the interval lengths on a log-log plot. A stan-  
192 dard linear regression to this plot will have a slope indicating the fractional  
193 Gaussian noise Hurst exponent  $H_{fGn}$ , and the spectral index is found by  
194  $\beta = 2H_{fGn} - 1$  (Eke et al., 2002).

195 *3.1.2. Scaled Window Variance*

196 For evaluating processes by scaled window variance, we refer the method  
197 proposed by Cannon, et al (Eke et al., 2002; Delignieres et al., 2006; Cannon  
198 et al., 1997; Bassingthwaighte and Raymond, 1999). Similar to dispersional  
199 analysis, the variance is found on increasing sized intervals of the signal. This  
200 method introduced a modification to remove local trends on each interval.  
201 In this method, bridge detrending is implemented to remove the local trend.  
202 The data in each interval is detrended by subtracting the “bridge”, a line  
203 connecting the first and last points in the interval. Then, the standard  
204 deviation is calculated for each detrended interval. Finally, the standard  
205 deviation of each interval is plotted versus the interval size on a log-log plot.

206 A standard linear regression to this plot will have a slope indicating the  
207 fractional Brownian motion Hurst exponent  $H_{fBm}$ , and the spectral index  
208 is found by  $\beta = 2H_{fBm} + 1$  (Eke et al., 2002).

### 209 3.1.3. Detrended Fluctuation Analysis

210 The approach for calculating the fractal index by detrended fluctuation  
211 analysis (DFA) is provided by Peng, et al (Peng et al., 1995b,a, 1994), and it  
212 has been thoroughly evaluated by others for many applications (Kantelhardt  
213 et al., 2002; Bryce and Sprague, 2012; Bardet and Kammoun, 2008; Caccia  
214 et al., 1997; Chen et al., 2002; Heneghan and McDarby, 2000; Hu et al.,  
215 2001; Kantelhardt et al., 2001; Schepers et al., 1992; Willson and Francis,  
216 2003). DFA calculates the proposed “scaling exponent”  $\alpha$  which is a useful  
217 to indicate the randomness of a time series over the boundary between fGn  
218 and fBm processes. The spectral index  $\beta$  is related to the DFA parameter  
219  $\alpha$  by (Eke et al., 2002)

$$\beta = 2\alpha - 1 \quad (4)$$

220 Implemented here is general scheme where the smallest interval is restricted  
221 to  $[\frac{N}{100}, 10]$  and the largest interval to  $[\frac{N}{10}, 20]$ .

### 222 3.2. Frequency Domain

223 These techniques directly evaluate the power law scaling property of a  
224 fractal series’ power spectral density. There are many available methods for  
225 performing the spectral estimation required to evaluate a fractal process’s  
226 frequency domain  $1/f^\beta$  power law (Pilgram and Kaplan, 1998; Heneghan  
227 and McDarby, 2000; Fougere, 1985). Here, the periodogram method and  
228 Eke’s  $lowPSD_{we}$  method are implemented (Eke et al., 2000, 2002; Delignieres  
229 et al., 2006). The periodogram method is used in calculating  $S(f)$ , the

230 square of the FFT after applying a Gaussian window. Eke improved on this  
231 method to more accurately characterize  $\beta$  for both signal classes. First, for  
232 the time series mean is subtracted, a parabolic window applied, and a bridge  
233 line connecting the first and last point of the signal is subtracted from the  
234 series. After calculating the power spectral density by the periodogram, all  
235 frequency estimates for  $f < 1/8f_{max}$  are omitted. Again,  $\beta$  is found by  
236 linear regression of the log-log power spectral density (Eke et al., 2002).

### 237 3.3. Time-Scale Domain

238 Proposed time-scale techniques by the wavelet transform are implemented  
239 (Eke et al., 2002; Audit et al., 2002; Jones et al., 1999; Simonsen et al., 1998;  
240 Veitch and Abry, 1999; Arneodo et al., 1996). The Average Wavelet Coeffi-  
241 cient (AWC) method described by Simonsen and Hansen (Simonsen et al.,  
242 1998) is conveniently implemented for this function. For the continuous  
243 wavelet transform of signal where in this case a twelfth order Daubechies  
244 wavelet is used (Simonsen et al., 1998). The number of levels for the Mallat  
245 algorithm discrete wavelet transform is chosen with respect to the signal  
246 length, determined here as never lower than  $2^3$  or greater than  $2^7$  (Mallat,  
247 1989). The result of the transformation provides the scale and transpose  
248 coefficients for the signal at the each of the prescribed levels. To find the  
249 averaged wavelet coefficient, the arithmetic mean with respect to the trans-  
250 lation coefficient is calculated. The average coefficients versus the levels are  
251 plotted on a log-log plot. A standard linear regression to this plot will have  
252 a slope  $H_{fBm} + \frac{1}{2}$ , and the spectral index is found by  $\beta = 2H_{fBm} + 1$  (Eke  
253 et al., 2002).

## 254 4. Evaluation of Algorithms

### 255 4.1. Discrete $1/f^\beta$ Process Generation

256 The first step in the analysis was the generation of a  $1/f^\beta$  fractal process.  
257 Li, et al proposed a method to create a filter of fractional order for generating  
258 fBm fractal processes by stochastically fractional differential equations (Li,  
259 2010; Li and Lim, 2006; Li and Chen, 2009). Kasdin extended this method  
260 for a generalized fractional filter inclusive of fGn and fBm signals, or  $1/f^\beta$   
261 processes (Kasdin, 1995). This method was implemented for this numerical  
262 analysis of  $1/f^\beta$  processes. The transfer function of the fractional system  
263 that follows the power law of  $\beta$  is given by

$$h(n) = \frac{\Gamma(\beta/2 + n)}{n!\Gamma(\beta/2)} \quad (5)$$

264 The realization of the process  $x(n)$  is found by the convolution operation

$$x(n) = w(n) * h(n) \quad (6)$$

265 where  $w(n)$  is randomly generated Gaussian white noise.

### 266 4.2. Numerical Analysis of Simulated Data Sets

267 The basis of this computational evaluation is the generation of  $1/f^\beta$   
268 power law processes. For completeness,  $\beta$  is calculated for all possible Hurst  
269 exponents in fGn and fBm classes for a total range  $-1 \leq \beta \leq 3$ . This is inclu-  
270 sive of fractional Gaussian noise and fractional Brownian motion processes  
271 for  $0 < H < 1$ . However, the anti-correlated fGn ( $\beta < 0$ ) and persistent fBm  
272 ( $\beta > 2$ ) regime signals are not be a matter of serious consideration in regard  
273 to physiological processes. The methods are evaluated over a range of time  
274 series lengths in order to observe the relationship between signal length and  
275 calculation accuracy for each fractal method. Given the length limitations

276 of previously recognized physiological data sets, time series lengths of 50,  
277 100, 200, 400, 600, 800, 1,000, 2,500, 5,000, 7,500, and 10,000 points are  
278 considered. Given the stochastic nature of these processes, the procedure of  
279 signal generation and calculation is implemented in a Monte Carlo scheme,  
280 where each realization is repeated 1,000 times. In each iteration for a set  
281 signal length, the time series is normalized and evaluated by each of the  
282 methods. Next, and a unit mean offset is added, and this signal reevaluated  
283 by each method. Then the mean of the series is subtracted from the offset  
284 series, resulting in a zero mean signal, and reevaluated. These three cases  
285 are calculated for each signal length for 1,000 realizations, and the mean  
286 value of  $\beta$  from each estimation is calculated. This computational scheme  
287 is the basis of the theoretical qualification of the fractal characterization  
288 algorithms, with strong consideration of the two recognized constraints of  
289 signal length and mean. Over the range of  $\beta$ , processes of the given length  
290 are generated for  $[-1, 3]$  incremented by 0.01.

#### 291 *4.3. Numerical Analysis of Stride Interval Data Sets*

292 Lastly, the published data sets are re-examined. First considered are  
293 right foot gait stride interval time series from normal subjects, consistent  
294 with previous investigation by Hausdorff, et al in the study of long range cor-  
295 relations in stride interval fluctuations (Hausdorff et al., 1996) and reconsid-  
296 ered by Deligieneras (Delignieres and Torre, 2009). Each of 10 healthy adult  
297 subjects walked at a self selected slow, normal, and fast pace, providing 30  
298 total time series. This study, henceforth referred to as Study I, implemented  
299 a power spectral analysis and DFA to find  $\beta$  and  $\alpha$  respectively (Hausdorff  
300 et al., 1996) to qualify and compare each method for fractal dynamics in  
301 gait. The mean time series length for the ten healthy control subjects is

302 3,179 points. Given the signals' significant length, these are considered to  
 303 be a basis set for evaluating the algorithm performance under sufficiently  
 304 long signal lengths. For consistency with the previous investigations, only  
 305 the first 2,048 points are used for calculation.

306 The second set comes from an investigation of gait dynamics in neurode-  
 307 generative diseases. The data was obtained by Hausdorff, et al in investiga-  
 308 tions of healthy and pathological correlations in stride interval time series  
 309 (Hausdorff et al., 2000, 1997, 1996). The signal lengths are considerably  
 310 constrained due to the physical limitations of the subject. An example of  
 311 healthy and pathological (ALS) time series provided by Studies I and II are  
 312 shown in Figure 3 with their corresponding PSDs and regression lines.

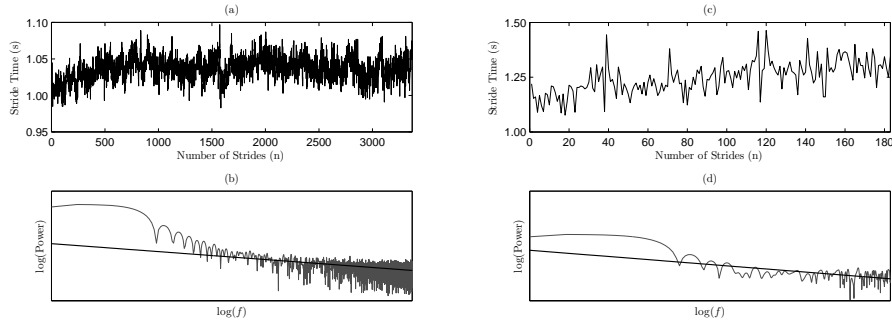


Figure 3: Sample stride interval time series and the corresponding PSDs:  
 (a) Study I (healthy) time series; (b) PDS of Study I (healthy) sample  
 time series; (c) Study II (ALS) time series; and (d) PSD of Study II (ALS)  
 time series.

313 In the investigation henceforth referred to as Study II,  $\alpha$  was calculated  
 314 by DFA. To again retain consistency with the previous investigation, only  
 315 the right foot stride interval time series is considered for calculation. Listed



316 in Table 1 are the total number and mean length of time series for each  
 317 of the cases of pathology and the control. The evaluation here is aimed to  
 318 demonstrate the algorithm performance in the regime of short time series.

Table 1: Number of time Series and mean length, Study II. ALS =  
 Amyotrophic Lateral Sclerosis, HD = Huntington’s Disease, PD =  
 Parkinson’s Disease, CO = Control.

	ALS	HD	PD	CO
<b>Number of Series</b>	13	20	15	16
<b>Mean Length</b>	196	242	184	255

319 For Study I, we fit a linear mixed model with estimated beta coefficient  
 320 as the dependent variable; walking speed, calculation method and their in-  
 321 teraction as fixed effects; and a participant random effect (Table 2). For  
 322 Study II, we fit a similar model with participant group, calculation method  
 323 and their interaction as fixed effects (Table 3). We used appropriately con-  
 324 structed means contrasts to obtain statistical significance of between-method  
 325 comparisons of interest.

## 326 5. Results

327 Presented in this section are the results of the numerical analysis scheme.  
 328 Secondly, the results from the evaluation of the published physiological data  
 329 sets of long time series from healthy individuals and shorter time series of  
 330 neurodegenerative disease subjects are examined. From the results of the  
 331 numerical analysis, this paper seeks to indicate which of the estimators can  
 332 most effectively evaluate fractal nature of the physiological time series under  
 333 the various constraints. The importance of accurately measuring  $\beta$  of the

334 physiological time series is also presented in this section, so the calculations  
 335 of the physiological data are compared with previously published results.

336 *5.1. Overall Theoretical Performance*

337 Considered first is the estimation accuracy of the algorithms for  $-1 \leq$   
 338  $\beta \leq 3$ . This presents the performance of the general scheme, which calculates  
 339 the mean spectral index  $\beta$  of 1,000 random fractal signals of lengths varying  
 340 from 50 to 10,000 points. This is under a normalized condition. Shown are  
 341 the mean-square error (MSE) of the estimators on the range  $-1 \leq \beta \leq 3$  for  
 342 signal lengths of of 100 and 10,000 points in Figure 4(a) and (b), respectively.

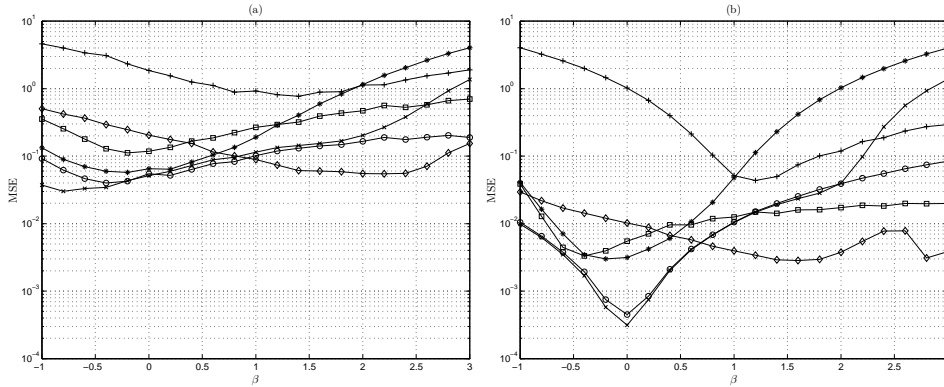


Figure 4: MSE vs  $\beta$ : (a)  $n = 100$  points; (b)  $n = 10,000$  points.  $\diamond$  AWC;  $+$  bdSWV;  $\square$  DFA;  $*$  Disp;  $\times$  PSD;  $\circ$   $low PSD_{we}$ .

343 The results of the analysis indicate that some estimators are indeed not  
 344 class independent. Figure 4(a) shows the MSE of the estimators on the  
 345 range  $-1 \leq \beta \leq 3$  for signal length of 100. For a short signal length, it  
 346 is clear that bdSWV and dispersional analysis estimators are fBm and fGn  
 347 class dependent, respectively. The bdSWV method exhibits very high MSE  
 348 for the fGn class ( $\beta < 1$ ) and dispersional analysis shows high MSE for all

349 fBm class signals ( $\beta > 1$ ). Similar error in the fGn class is noted for the  
 350 AWC method, and the error decreases for  $\beta > 1$ . DFA exhibits relatively  
 351 high MSE values for both fBm and fGn processes with a relatively flat  
 352 profile on this range. However, DFA demonstrates slightly greater accuracy  
 353 than AWC method for signals close to white Gaussian fGn signals. Both  
 354 power spectral density methods, the periodogram (PSD) and the modified  
 355 method  $^{low}PSD_{we}$  show quite consistent accuracy for all signal classes with  
 356 a relatively flat MSE profile across the range of  $\beta$ . Interestingly, for short  
 357 signal lengths, the basic periodogram (PSD) method is more accurate than  
 358 the  $^{low}PSD_{we}$  method. However, the MSE of the PSD increases significantly  
 359 for persistent fBm type signals ( $\beta > 2$ ).

360 Considering the case of long time series length of 10,000 points given in  
 361 Figure 4(b) it is clear that the bdSWV method has significantly high MSE  
 362 for all fGn class signals ( $\beta < 1$ ). Similarly, dispersional analysis demon-  
 363 strates high MSE for all fBm class signals ( $\beta > 1$ ). AWC shows relatively  
 364 consistent MSE for both classes, though the MSE decreases as the signal  
 365 type approaches Brownian motion ( $\beta = 2$ ). There is though an observable  
 366 MSE increase for persistent fBm signals. DFA similarly demonstrates class  
 367 independent behavior, with lower MSE for fGn class signals. Again in the  
 368 long signal length case, DFA indicates DFA exhibits a relatively consistent  
 369 MSE in both the fGn and fBm class. Both power spectral density methods,  
 370 the periodogram (PSD) and the modified method  $^{low}PSD_{we}$  demonstrate  
 371 similar MSE, which is lowest for white Gaussian noise fGn processes. Higher  
 372 MSE is observed for fBm class signals, though the error is not as high as in  
 373 the class dependent dispersional and bdSWV methods. The modified PSD  
 374 method shows higher accuracy than the standard periodogram for persistent  
 375 fBm type signals ( $\beta > 2$ ).

376 Given the clear relationship of the MSE and the signal length, examined  
 377 next is the MSE value over a range of signal lengths. Each value is the  
 378 1,000 realization ensemble mean MSE for the given length. For conciseness,  
 379 anti-correlated fGn ( $\beta = -1$ ) and persistent fBm ( $\beta = 3$ ) evaluations are  
 380 excluded. Shown in Figure 5(a) is the mean-square error (MSE) of the  
 381 estimators on the range  $50 \leq N \leq 10,000$  for white Gaussian noise fGn  
 382 signals of  $\beta = 0$ .

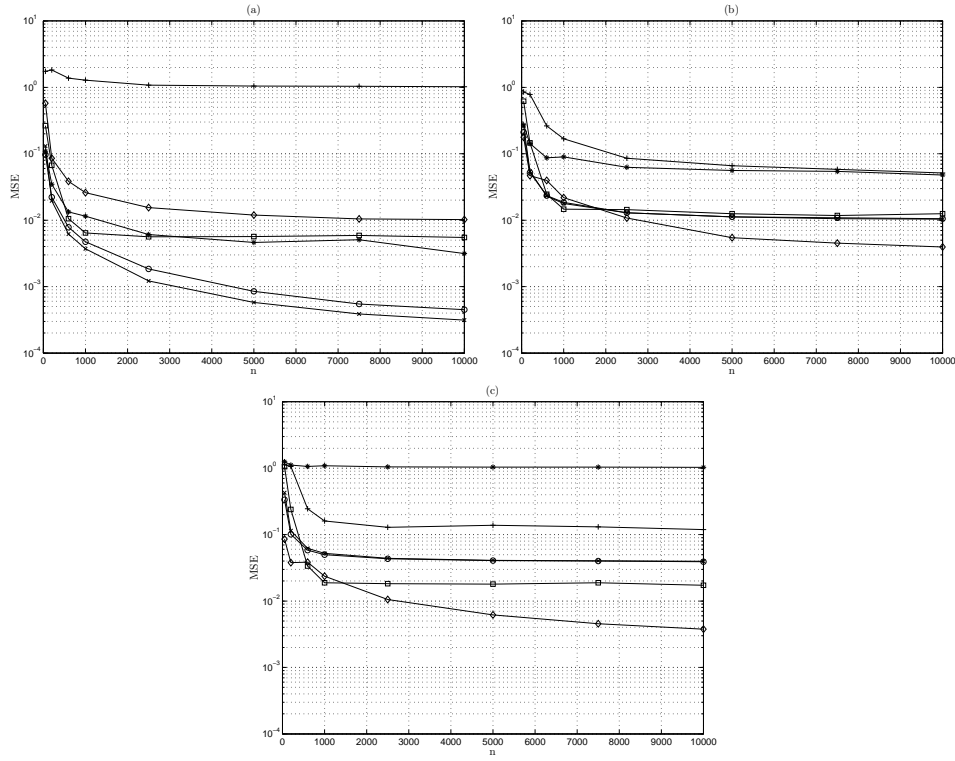


Figure 5: MSE vs n: (a)  $\beta = 0$ ; (b)  $\beta = 1$ ; (c)  $\beta = 2$ .  $\diamond$  AWC;  $+$  bdSWV;  
 $\square$  DFA;  $*$  Disp;  $\times$  PSD;  $\circ$   $low PSD_{we}$ .

383 For the white Gaussian noise case of fGn class signals  $\beta = 0$ , the MSE  
 384 of the bdSWV method is high regardless of signal length. The MSE for

385 dispersive analysis decreases as signal length increases, and at long signal  
386 length is among of the most accurate estimators for this signal class. In-  
387 terestingly, DFA shows diminishing returns in accuracy beyond  $N = 1,000$ .  
388 AWC consistently shows increasing accuracy as signal length increases. For  
389 the white Gaussian case of fGn signals, the power spectral density meth-  
390 ods again exhibit the lowest overall MSE which decreases for greater signal  
391 length.

392 The mean-square error of the estimators on the range  $50 \leq N \leq 10,000$   
393 is observed in the critical case of the boundary of fGn and fBm signals for  
394  $1/f^\beta$  processes of  $\beta = 1$ . Here, it is expected to see that regardless of signal  
395 length, both class dependent methods bdSWV and dispersive analysis  
396 exhibit crossover and a similar order of MSE. DFA shows initially high  
397 MSE that decreases as signal length increases, though again with quickly  
398 diminishing returns. The power spectral density methods show a similar  
399 profile. AWC again shows increasing accuracy as the length is increased. For  
400 shorter length signals cases, the MSE of AWC, DFA, and spectral methods  
401 are clustered closely together.

402 The third case consideration is the MSE versus length for Brownian  
403 motion fBm signals of  $\beta = 2$ . For the Brownian motion process indicative of  
404 the fBm class, the MSE of dispersive analysis is high regardless of signal  
405 length, indicating its class dependence. The MSE of bdSWV is lower than  
406 in the fGn class, though it is still significantly greater than other methods.  
407 DFA reaches its maximum accuracy at  $N = 1,000$  points. AWC exhibits  
408 the sharpest drop off in error of all methods, and regardless of signal length  
409 has generally the lowest error for Brownian motion fBm class signals. The  
410 spectral methods show low MSE for very short time series, but quickly  
411 diminishing returns for signals greater than 1,000 points.

412 Considering the class dependence of the bdSWV and dispersional analy-  
 413 sis methods, subsequent observations of the results will not consider findings  
 414 for these methods. This is in the interest of determining a robust class inde-  
 415 pendent estimator. Accordingly,  $^{low}PSD_{we}$  is considered class independent  
 416 for its modifications which allow a more accurate estimation of fBm pro-  
 417 cesses than the unmodified periodogram method. In conclusion, further  
 418 elaborations on the MSE, mean error (ME), and standard deviation (SD) of  
 419 techniques will consider DFA,  $^{low}PSD_{we}$ , and AWC.

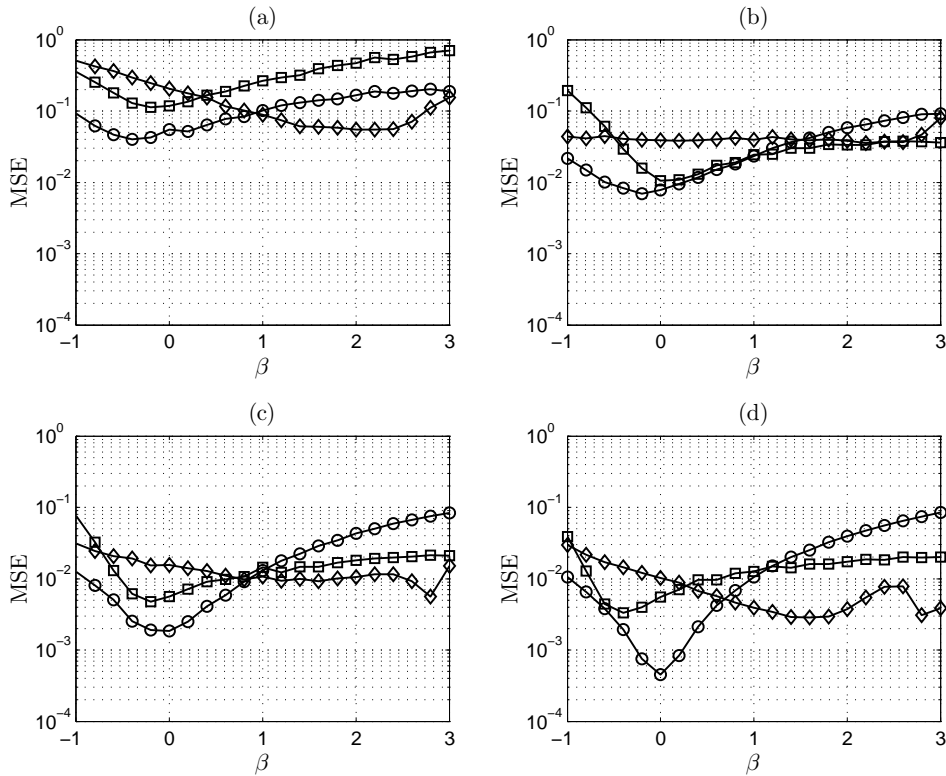


Figure 6: MSE vs  $\beta$ : (a)  $n = 100$  points; (b)  $n = 600$  points; (c)  $n = 2,500$  points; and (d)  $n = 10,000$  points.  $\diamond$  AWC;  $\square$  DFA;  $\circ$   $^{low}PSD_{we}$ .

420 Figure 6 shows the mean-square error of the estimators DFA,  $^{low}PSD_{we}$ ,

421 and AWC on the range  $-1 \leq \beta \leq 3$  for signal length of 100, 600, 2,500, and  
 422 10,000. For the two short series sets ( $N = 100$ ,  $N = 600$ ), all methods  
 423 exhibit a relatively consistent profile of MSE over the entire range of  $\beta$ . For  
 424 short time series, AWC is most accurate in the fBm class, and  $^{low}PSD_{we}$  is  
 425 most accurate in the fGn class. DFA is generally less accurate than AWC and  
 426  $^{low}PSD_{we}$ . Though DFA may be more accurate than AWC at estimating a  
 427 white Gaussian fGn process, the accuracy of  $^{low}PSD_{we}$  is still preferable. A  
 428 similar observation can be made in longer time series of length 600, 2,500,  
 429 and 10,000. DFA shows preferable performance to AWC near white Gaussian  
 430 noise, and here the accuracy of  $^{low}PSD_{we}$  is always favorable. An important  
 431 characteristic of AWC is its relatively flat MSE over the range of  $\beta$  for all  
 432 signal lengths. A notable increase in MSE exists for  $^{low}PSD_{we}$  in the fBm  
 433 class as the length is increased, due to the effects of more low frequency  
 434 content in these signals.

435 The definition of MSE necessarily combines the bias and variance into  
 436 one value. To distinguish the individual effects of bias and variance in the  
 437 notion of the estimators' MSE on this range, the bias (mean error) and  
 438 variance (standard deviation) will be examined separately in the following  
 439 figures. Figure 7 shows the mean error (ME) of AWC,  $^{low}PSD_{we}$ , and DFA  
 440 on the range  $-1 \leq \beta \leq 3$  for signal lengths of 100, 600, 2,500, and 10,000.

441 Figure 7 indicates that for short time series, the MSE of AWC is largely  
 442 influenced by bias. This effect is diminished in the fBm regime. The mean  
 443 error of DFA is lower than  $^{low}PSD_{we}$  and AWC for the fGn class. The  
 444 MSE of DFA is consistently influenced by bias in the fBm range.  $^{low}PSD_{we}$   
 445 exhibits less overall fluctuation, and estimation bias increases with  $\beta$ . This  
 446 is likely due to the influence of more low frequency components when eval-  
 447 uating the linear regression of the power spectral density. For subsequently

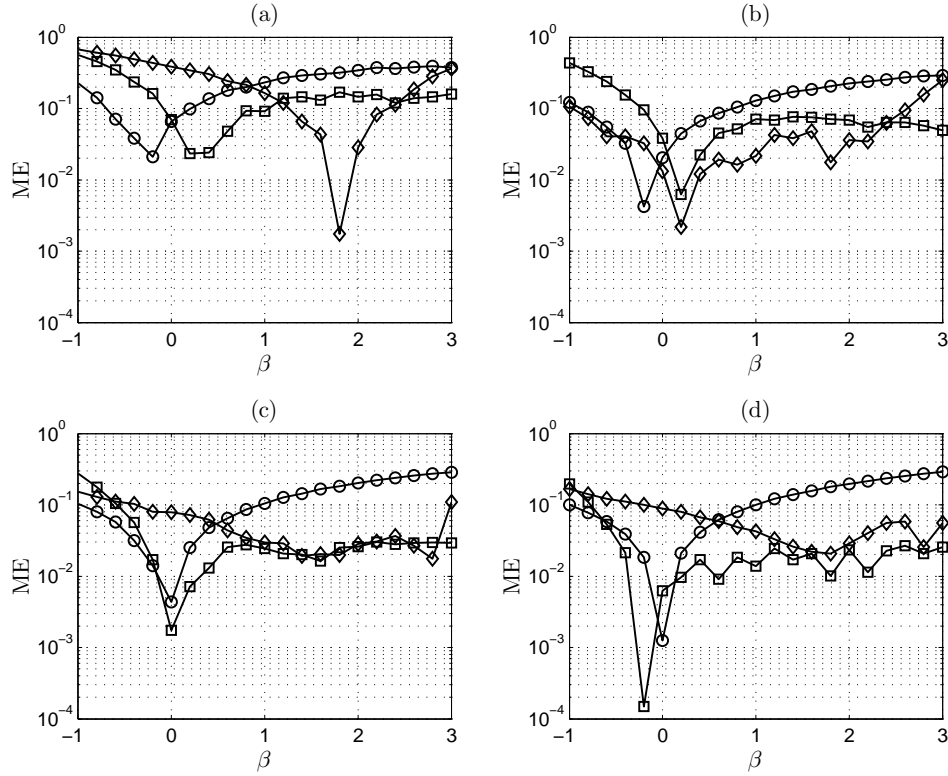


Figure 7: ME vs  $\beta$ . (a)  $n = 100$  points; (b)  $n = 600$  points; (c)  $n = 2,500$  points; and (d)  $n = 10,000$  points.  $\diamond$  AWC;  $\square$  DFA;  $\circ$   $low PSD_{we}$ .

448 longer signal lengths of 600, 2,500, and 10,000, the bias effects on the MSE  
 449 of DFA and AWC are comparable beyond  $\beta = 0$ .

450 Figure 8 shows the standard deviation ( $\sigma$ ) of DFA,  $low PSD_{we}$ , and AWC  
 451 on the range  $-1 \leq \beta \leq 3$  for signal length of 100, 600, 2,500, and 10,000.  
 452 For short signal length, the standard deviation of DFA is significant. The  
 453 standard deviation of  $low PSD_{we}$  and AWC are very consistent on the range  
 454 of  $\beta$ .  $low PSD_{we}$  shows the overall lowest standard deviation for both signal  
 455 classes for all signal lengths. For longer signal lengths, the standard devi-  
 456 ation profile of DFA is relatively unchanged. The profile of AWC is flat in



457 each case, with increasing accuracy with signal length. DFA exhibits lower  
 458 standard deviation than AWC for fGn class signals of length 600 and 2,500,  
 459 though the accuracy of  $^{low}PSD_{we}$  is still preferential.

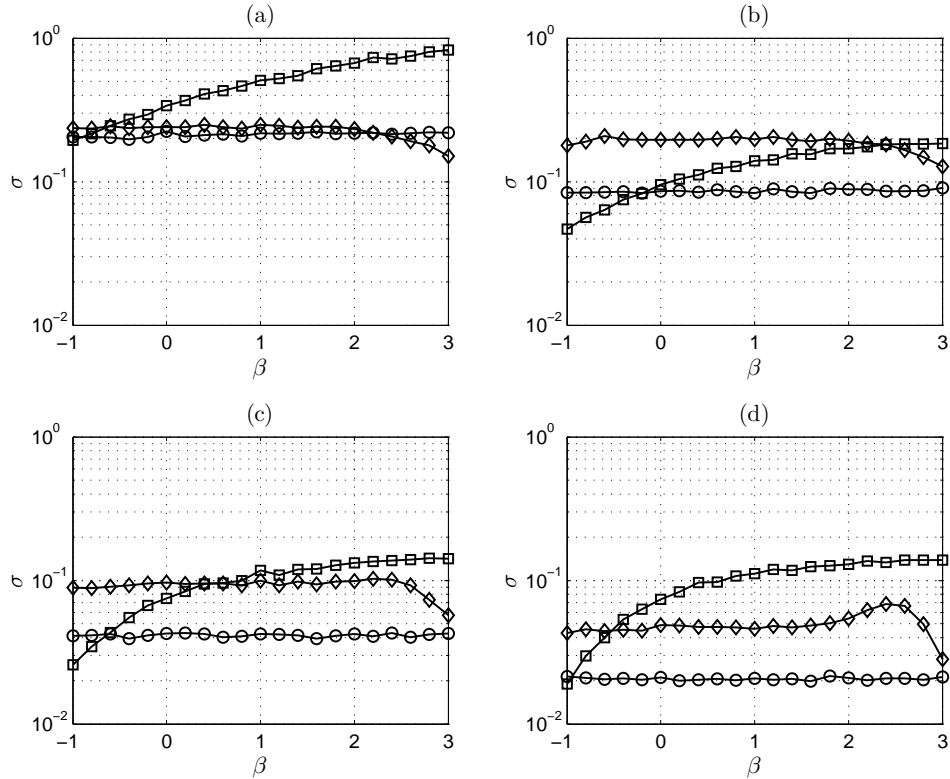


Figure 8:  $\sigma$  vs  $\beta$ : (a)  $n = 100$  points; (b)  $n = 600$  points; (c)  $n = 2,500$  points; and (d)  $n = 10,000$  points.  $\diamond$  AWC;  $\square$  DFA;  $\circ$   $^{low}PSD_{we}$ .

## 460 5.2. Effects of Nonzero Mean

### 461 5.2.1. Added Unit Mean

462 Presented in this section are findings for realizations of the algorithms for  
 463 the complete range  $-1 \leq \beta \leq 3$  on an extension of the previously described  
 464 scheme where a the signal is normalized and unit mean is added. Figure

465 9 (a) and (b) show the mean-square error of the estimators on the range  
 466  $-1 \leq \beta \leq 3$  for biased signal length of 100 and 10,000, respectively.

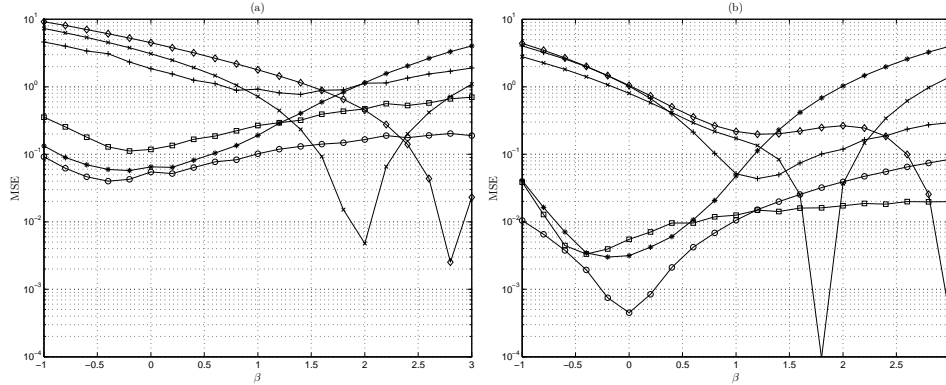


Figure 9: MSE vs  $\beta$ , added unit mean: (a)  $n = 100$  points; (b)  $n = 10,000$  points.  $\diamond$  AWC;  $+$  bdSWV;  $\square$  DFA;  $*$  Disp;  $\times$  PSD;  $\circ$   $^{low}PSD_{we}$ .

467 Compared to the original normalized signal condition shown in Figure  
 468 9, the additional unit mean affects only the MSE of the frequency and time-  
 469 scale domain methods. The adjustments introduced to the power spectral  
 470 density method by  $^{low}PSD_{we}$  avoid the error effects of nonzero mean. It  
 471 is critical to note that a significant DC component from a series mean will  
 472 largely influence a low frequency range of the power spectral density, and  
 473 subsequently the linear regression estimation for the spectral estimators.  
 474 However, the constant unit mean has diminishing influence on increasingly  
 475 non-stationary processes, and thus the effect is diminished as  $\beta$  increases.  
 476 This observation is reflected in the findings of the dependence of the MSE  
 477 on signal length with nonzero mean. Inaccuracy in the AWC method is  
 478 significantly influenced in the fGn class, and error is still generally present  
 479 for all fGn and fBm class signals. The nonzero mean has no effect on the  
 480 time domain methods.

481 5.2.2. Removal of Mean

482 Finally observed is the estimation accuracy when the series mean is re-  
 483 moved. These results are from the third extension of the numerical analysis  
 484 scheme. From the second case where the signal is normalized and unit mean  
 485 is added, the mean of the resulting signal is calculated and subtracted from  
 486 the time series. Shown in Figure 10 (a) and (b) are the mean-square error  
 487 of the estimators on the range  $-1 \leq \beta \leq 3$  for a zero mean signal length of  
 488 of 100 and 10,000, respectively.

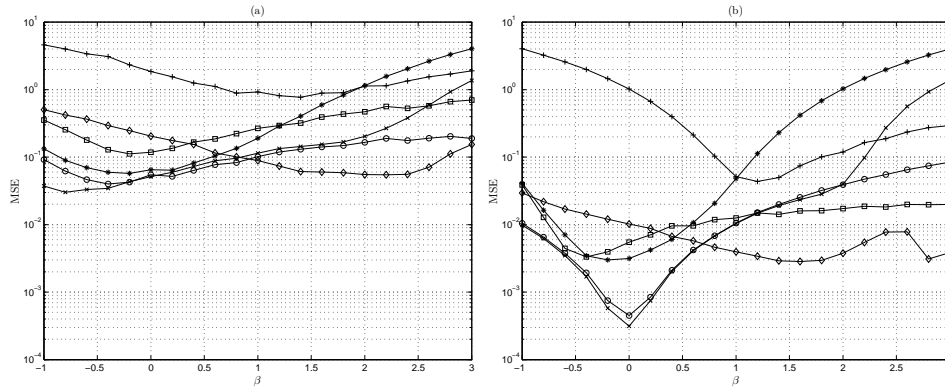


Figure 10: MSE vs  $\beta$ , zero mean: (a)  $n = 100$  points; (b)  $n = 10,000$  points.  $\diamond$  AWC;  $+$  bdSWV;  $\square$  DFA;  $*$  Disp;  $\times$  PSD;  $\circ$   $^{low} PSD_{we}$ .

489 Figure 10 indicates that when the mean is removed by simply subtracting  
 490 the mean value of the series, the estimation accuracy returns to the original  
 491 profile. Thus, removing the series mean is valid to avoid errors in series  
 492 estimation by methods which are sensitive. The original mean square error,  
 493 mean error, and standard deviation profiles are realized when the series  
 494 mean is removed and the series is reevaluated.

495 5.3. Gait Stride Interval Analysis

496 This section presents the results of the application of these techniques  
 497 to experimentally measured gait stride interval time series. To keep the  
 498 analysis concise, the methods implemented were those of the lowest MSE  
 499 from each domain class. Thus,  $\beta$  was calculated by DFA,  $^{low}PSD_{we}$ , and  
 500 AWC. For the AWC calculation, the preprocessing step of mean removal  
 501 is performed. For a thorough evaluation of Study I,  $\beta$  is calculated and  
 502 converted to  $\alpha$  by the relationship  $\alpha = \frac{\beta+1}{2}$ . For clarity, these calculated  
 503 values of  $\beta$  and  $\alpha$  are presented separately in Table 2, showing the values  
 504 (*mean  $\pm$  standard deviation*) from the study and our calculations for DFA,  
 505  $^{low}PSD_{we}$ , and AWC. Furthermore, the calculated values were statistically  
 506 different ( $p < 0.03$ ) among the used approaches, except between AWC and  
 507 DFA for fast and normal walks ( $p > 0.07$ ).

Table 2: A comparative analysis of the algorithms for time series from  
 Study I.

		$\beta$			$\alpha$		
		Slow	Normal	Fast	Slow	Normal	Fast
Study I	DFA	0.96 $\pm$ 0.13	0.80 $\pm$ 0.07	0.94 $\pm$ 0.09	0.98 $\pm$ 0.07	0.90 $\pm$ 0.04	0.97 $\pm$ 0.05
	PSD	1.01 $\pm$ 0.15	0.81 $\pm$ 0.09	0.94 $\pm$ 0.07	1.01 $\pm$ 0.08	0.91 $\pm$ 0.05	0.97 $\pm$ 0.04
Analysis	DFA	0.93 $\pm$ 0.13	0.77 $\pm$ 0.15	0.94 $\pm$ 0.17	0.97 $\pm$ 0.07	0.88 $\pm$ 0.08	0.97 $\pm$ 0.09
	$^{low}PSD_{we}$	0.73 $\pm$ 0.15	0.48 $\pm$ 0.09	0.62 $\pm$ 0.17	0.87 $\pm$ 0.08	0.74 $\pm$ 0.05	0.81 $\pm$ 0.09
	AWC	1.07 $\pm$ 0.17	0.87 $\pm$ 0.10	1.00 $\pm$ 0.18	1.03 $\pm$ 0.09	0.94 $\pm$ 0.05	1.00 $\pm$ 0.09

508 Considered next are calculations for shorter time series of pathological  
 509 gait conditions from Study II. Due to the physical limitations of the patients  
 510 under investigation, the shortness of the time series length given in Table  
 511 1 is noted when considering the results of these calculations. Again, the  
 512 spectral index  $\beta$  is calculated by DFA,  $^{low}PSD_{we}$ , and AWC and converted

513 to the DFA scaling exponent  $\alpha$ . The series mean has been removed for  
514 calculation by AWC. Table 3 shows the published and calculated values  
515 (*mean  $\pm$  standard error*) of  $\beta$  and the corresponding of  $\alpha$  for the calculations  
516 by DFA,  $^{low}PSD_{we}$ , and AWC methods. Furthermore, the AWC values were  
517 statistically different from the values calculated by DFA and  $^{low}PSD_{we}$  ( $p <$   
518  $0.04$ ) in all cases. However, the values calculated by DFA and  $^{low}PSD_{we}$   
519 were not statistically different in any of the cases ( $p > 0.09$ ).

Table 3: A comparative analysis of the algorithms for time series from  
Study II.

		$\beta$				$\alpha$			
		ALS	HD	PD	CO	ALS	HD	PD	CO
Study II	DFA	0.48 $\pm$ 0.13	0.20 $\pm$ 0.07	0.64 $\pm$ 0.11	0.82 $\pm$ 0.09	0.74 $\pm$ 0.07	0.60 $\pm$ 0.04	0.82 $\pm$ 0.06	0.91 $\pm$ 0.05
	DFA	0.66 $\pm$ 0.13	0.37 $\pm$ 0.12	0.52 $\pm$ 0.16	0.60 $\pm$ 0.10	0.83 $\pm$ 0.07	0.68 $\pm$ 0.06	0.76 $\pm$ 0.08	0.80 $\pm$ 0.05
Analysis	$^{low}PSD_{we}$	0.56 $\pm$ 0.08	0.26 $\pm$ 0.09	0.39 $\pm$ 0.11	0.49 $\pm$ 0.05	0.78 $\pm$ 0.04	0.63 $\pm$ 0.05	0.70 $\pm$ 0.06	0.74 $\pm$ 0.03
	AWC	0.97 $\pm$ 0.10	0.54 $\pm$ 0.13	0.73 $\pm$ 0.15	0.94 $\pm$ 0.06	0.98 $\pm$ 0.05	0.78 $\pm$ 0.06	0.87 $\pm$ 0.08	0.97 $\pm$ 0.03

## 520 6. Discussion

### 521 6.1. Simulated Signals

522 From the results of the theoretical evaluation of these techniques, dis-  
523 tinct limitations and benefits of each of the methods can be observed. When  
524 determining an appropriate technique to evaluate the fractal nature of a pro-  
525 cess, it is critical to consider the time series length, any apparent mean, and  
526 in some cases the range on which the process's spectral index might exist. It  
527 is therefore apparent from our analysis that making a conclusion about the  
528 fractal nature of short physiological time series can be quite tenuous. The  
529 nature of physiological data sets and their relationship to ideal  $1/f^\beta$  profiles

530 should be a significant consideration when drawing conclusions about the  
531 results of these analyses.

532 In the interest of determining class independent estimators, the dis-  
533 persional and bdSWV methods are clearly not viable. Though developed  
534 for consideration of fGn and fBm class signals respectively, these methods  
535 can provide incorrect results for signals typical of physiological processes at  
536  $\beta = 1$ . The recommendation to favor class independent methods is to effec-  
537 tively reduce the burden of determining the signal class before evaluation.  
538 DFA is a candidate, as it indicates no preferential performance in either  
539 class. Additionally, the evaluation is unaffected by a non-zero series mean.  
540 However, the results for DFA have significantly large mean-square error and  
541 standard deviation for short time series (Bryce and Sprague, 2012). It is  
542 apparent that DFA has little utility for short time series, and exhibits di-  
543 minishing returns in accuracy for longer series, as other investigations have  
544 observed (Delignieres et al., 2006; Bryce and Sprague, 2012; Bardet and  
545 Kammoun, 2008).

546 A significant limitation of the frequency domain methods is the effect of  
547 low frequencies and DC on the accuracy of these methods. Indeed, a the  
548 critical property of fractal processes is that the power spectral density is  
549 not convergent for ( $\omega = 0$ ), and this presents some problems for analysis  
550 (Li, 2010). However, removing DC and low frequency content from the  
551 spectrum risks destroying low frequency information, and thus some scale  
552 invariant features of the process. Additionally, the significantly lower MSE  
553 observed in the spectral methods for white Gaussian fGn processes is likely  
554 an artifact of the time series generation by the same principle (Kasdin, 1995).  
555 Regardless, accurately estimating the properties of white Gaussian processes  
556 does not present any significant utility with respect to the interest of fractal

557 characterization of physiological processes, where a simple autocorrelation  
558 analysis or Lilliefors test may suffice.

559 AWC has a more uniform performance for the range of fGn and fBm  
560 class signals. Though AWC was significantly affected by non-zero mean  
561 signals, this effect is corrected by the removal of the time series mean be-  
562 fore evaluation. Unlike the modifications to spectral methods to eliminate  
563 ill-fitting due to DC or high frequency noise, this is a straightforward pre-  
564 processing step easily integrated with the main algorithm. This combination  
565 also provides intact frequency and scale dependent information of the series.  
566 DFA presents significant risk for short time series and provides no clear  
567 advantage in many instances, where  $^{low}PSD_{we}$  can likely provide a more  
568 accurate complement to AWC analysis. In general, given these two primary  
569 constraints of non-zero mean and short time series in gait stride interval  
570 signals, AWC can provide uniformly accurate characterization for short and  
571 long biased data series. Regardless, discretion of the desired precision and  
572 accuracy, illustrated by the mean error and standard deviation, is encour-  
573 aged in all applications. Generally, the MSE of all estimators indicate that  
574 AWC is a generally robust method, consistent under many circumstances  
575 and favorable especially under conditions of physiological interest.

## 576 6.2. Stride Intervals Time Series

577 The analysis of the physiologically extracted time series provides perhaps  
578 the most significant indication of the applicability of these methods in a  
579 physiological setting. Table 2 shows the fractal characterizations for long  
580 time series of ten healthy adults walking at self selected paces. In these  
581 time series, the mean amplitude is 0.2025 and the mean of the series is  
582 1.1481, indicative of the inherent non-zero mean offset. The effects of these

583 signal characteristics are observed in our evaluation of these time series by  
 584 DFA,  $^{low}PSD_{we}$ , and AWC. For the self selected slow, normal, and fast  
 585 time series, the DFA and AWC methods evaluate a mean spectral index of  
 586  $0.88 \pm 0.15$  and  $0.98 \pm 0.15$  respectively. To validate this disparity, consider  
 587 the results of the simulated time series for length of 100 and  $\beta = 1$ . The  
 588 MSE of AWC is preferable in this instance, and is exemplified by observing  
 589 the substantial standard deviation of DFA here. The underestimation of  
 590 the spectral index here by  $^{low}PSD_{we}$  is noted. Considering physiologically  
 591 meaningful conclusions from the pathological gait data is more difficult given  
 592 the inherently short length of the time series. These evaluations given by  
 593 Table 3 show the findings for short time series of ALS, Huntington’s Disease,  
 594 Parkinson’s Disease, and control subjects. For all series, the mean time series  
 595 length is 190 points. The mean amplitude is 0.2788 and the mean of the  
 596 series is 1.0866, again showing a non-zero mean offset. For pathological  
 597 gait time series, more stationary fGn type characteristics may be expected.  
 598 Given the MSE for  $\beta$  on the range of  $[0,1]$  for length of 100, the accuracy of  
 599 DFA, AWC, and  $^{low}PSD_{we}$  are generally comparable on the order of  $10^{-1}$ .  
 600 Table 3 still show disparity between each estimator, error largely affected  
 601 by the time series length.

602 The drastic underestimation of the spectral index by the frequency do-  
 603 main based method is observed in both studies. To avoid error in the es-  
 604 timation introduced by noise, the  $^{low}PSD_{we}$  necessitates removal of high  
 605 frequency components of  $1/8 * f_{max}$ . The underestimation of the spectral  
 606 index in the power spectrum indicates a greater effect of the high frequency  
 607 content of the signal, so this adjustment did not quite nullify the effects of  
 608 high frequency biasing. Though the MSE of AWC and DFA are similar,  
 609 the AWC method is similarly biased but has much lower standard devia-



610 tion. DFA on this range again presents significant standard deviation. This  
611 highlights the critical concern of the application of DFA to pathological time  
612 series of short length. It is therefore concluded here that the results provided  
613 by AWC are more tenable.

614 It is clear that DFA and spectral methods in many instances require  
615 extensive modification to properly assess the data. It is seen that necessity  
616 of such modifications as a potentially hazardous burden which could render  
617 results incorrect and obfuscate interpretations. Indeed, in the proposal of  
618 these methods for gait stride interval analysis by Hausdorff, the window  
619 sizes and fitting ranges for DFA and the frequency range for the spectral  
620 method linear regression required significant scrutiny to achieve a desired  
621 result (Hausdorff et al., 1996; Delignieres et al., 2006). In this case, the  
622 relationship between the scales of the significant physiological frequencies  
623 and noise frequencies can be inferred in a general sense. However, it is not  
624 always possible to make a clear distinction between noise and physiolog-  
625 ically meaningful frequency content in all physiological and experimental  
626 settings. DFA similarly requires adjustment of the bounds of window size.  
627 This adjustment can significantly impacts the final calculation, and varies  
628 between applications depending on the amplitude of fluctuations in the cho-  
629 sen window. This would require specific specialization of this method for  
630 each application. The risks and burdens of specialization of these methods  
631 can be effectively reduced given the generally favorable performance AWC.  
632 It is noted that the only requirement to avoid errors in AWC is preprocessing  
633 the signal by subtracting the mean.

## 634 7. Conclusions

635 The objective of this study was to provide a comparative analysis of frac-  
636 tal characterization algorithms of  $1/f^\beta$  time series with respect to physio-  
637 logical applications. Primarily, the numerical analysis allowed us to provide  
638 insight into the time series lengths and signal classes on which previously  
639 proposed algorithms returned acceptably accurate results. If fractal charac-  
640 teristics are of interest for some arbitrary physiological process, it is critical  
641 to choose a class independent algorithm with consistent accuracy and preci-  
642 sion. When signal class is not given a priori or classification is not possible,  
643 the application of class dependent estimators is not feasible. The evalua-  
644 tion of these algorithms, bdSWV and dispersional analysis, has shown that  
645 the limited utility of these methods in this setting. However, these are  
646 still relatively valid evaluations if a signal class can be determined. Once  
647 a process can be classified as fGn or fBm by a more robust consistent and  
648 accurate estimator such as AWC, a class specific estimator may provide a  
649 useful complementary analysis. In contrast to the findings under simulation,  
650 the inherent nature of experimentally derived physiological signals present  
651 further challenges in evaluating fractal properties. The sensitivity of power  
652 spectral methods to a non-zero mean and high frequency were observed, and  
653 necessitate the task of distinguishing the range of physiologically meaning-  
654 ful frequencies from noise. Similarly, the potential errors influenced in DFA  
655 from large local fluctuations in small window sizes are noted. However, the  
656 application of a method requires the recognition of several key characteris-  
657 tics of pathological gait time series. First, the understood composition and  
658 function of the locomotor system insists that the statistical properties of  
659 the gait outcome can be analyzed to have fractal properties. It has been

660 shown that aging and neurodegenerative diseases result in decreased central  
661 processing capabilities, proprioception, muscle strength and endurance, and  
662 significant dysfunction in motor neurons, the cerebral cortex, brain stem,  
663 and spinal cord. Accordingly, diminished function to any components of  
664 the locomotor system caused by aging or disease will affect these statistical  
665 outcomes and thus the fractal characteristic. Another key characteristic of  
666 pathological time series is the typically shortened length. In light of the  
667 results of the numerical analysis, the AWC method is recommended as a  
668 useful tool for measuring the fractal characteristic of time series. This is a  
669 useful tool which can more rapidly and accurately track functional changes  
670 in stride interval dynamics. Clinically, this translates to a biomarker of a  
671 potentially hidden pathology or decline due to disease or aging that can be  
672 quickly and reliably monitored and inform subsequent therapeutic interven-  
673 tion. A final advantage of this application recognized by the comparative  
674 evaluation of these algorithms is the relief of the burden of specific adjust-  
675 ments for each application. This numerical and corresponding gait stride  
676 interval physiological analyses provide a justifiable basis for the applications  
677 of AWC to a variety signals of interest for a more informative indicator of  
678 the fractal nature of these processes.

### 679 **Acknowledgment**

680 This work was supported in part by the Pittsburgh Claude D. Pepper  
681 Older Americans Independence Center (NIA P30 AG 024827).

682 **References**

- 683 Arneodo, A., d'Aubenton Carafa, Y., Bacry, E., Graves, P., Muzy, J., Ther-  
684 mes, C., 1996. Wavelet based fractal analysis of DNA sequences. *Physica*  
685 *D: Nonlinear Phenomena* 96 (1), 291–320.
- 686 Audit, B., Bacry, E., Muzy, J. F., Arneodo, A., 2002. Wavelet-based es-  
687 timators of scaling behavior. *IEEE Transactions on Information Theory*  
688 48 (11), 2938–2954.
- 689 Bak, P., Chen, K., 1991. Self-organized criticality. *Scientific American*  
690 264 (1).
- 691 Bardet, J. M., Kammoun, I., 2008. Asymptotic properties of the detrended  
692 fluctuation analysis of long-range-dependent processes. *IEEE Transac-*  
693 *tions on Information Theory* 54 (5), 2041–2052.
- 694 Bassingthwaighte, J. B., 1988. Physiological heterogeneity: fractals link de-  
695 terminism and randomness in structures and functions. *Physiology* 3 (1),  
696 5–10.
- 697 Bassingthwaighte, J. B., Bever, R. P., 1991. Fractal correlation in heteroge-  
698 neous systems. *Physica D: Nonlinear Phenomena* 53 (1), 71–84.
- 699 Bassingthwaighte, J. B., Raymond, G. M., 1994. Evaluating rescaled range  
700 analysis for time series. *Annals of Biomedical Engineering* 22 (4), 432–444.
- 701 Bassingthwaighte, J. B., Raymond, G. M., 1995. Evaluation of the disper-  
702 sional analysis method for fractal time series. *Annals of Biomedical Engi-*  
703 *neering* 23 (4), 491–505.

- 704 Bassingthwaighte, J. B., Raymond, G. M., 1999. Deriving dispersional and  
705 scaled windowed variance analyses using the correlation function of dis-  
706 crete fractional Gaussian noise. *Physica A: Statistical Mechanics and its*  
707 *Applications* 265 (1), 85–96.
- 708 Blin, O., Ferrandez, A.-M., Serratrice, G., 1990. Quantitative analysis of  
709 gait in Parkinson patients: increased variability of stride length. *Journal*  
710 *of the Neurological Sciences* 98 (1), 91–97.
- 711 Bryce, R. M., Sprague, K. B., 2012. Revisiting detrended fluctuation anal-  
712 ysis. *Scientific Reports* 2.
- 713 Caccia, D. C., Percival, D., Cannon, M. J., Raymond, G., Bassingthwaighte,  
714 J. B., 1997. Analyzing exact fractal time series: evaluating dispersional  
715 analysis and rescaled range methods. *Physica A: Statistical Mechanics*  
716 *and its Applications* 246 (3), 609–632.
- 717 Cannon, M. J., Percival, D. B., Caccia, D. C., Raymond, G. M., Bass-  
718 ingthwaighte, J. B., 1997. Evaluating scaled windowed variance methods  
719 for estimating the Hurst coefficient of time series. *Physica A: Statistical*  
720 *Mechanics and its Applications* 241 (3), 606–626.
- 721 Chen, Y., Ding, M., Kelso, J. A. S., 1997. Long memory processes  $1/f^\alpha$  type  
722 in human coordination. *Physical Review Letters* 79 (22), 4501–4504.
- 723 Chen, Z., Ivanov, P. C., Hu, K., Stanley, H. E., 2002. Effect of nonsta-  
724 tionarities on detrended fluctuation analysis. *Physical Review E* 65 (4),  
725 041107.
- 726 Crevecoeur, F., Bollens, B., Detrembleur, C., Lejeune, T., 2010. Towards  
727 a “gold-standard” approach to address the presence of long-range auto-

728 correlation in physiological time series. *Journal of Neuroscience Methods*  
729 192 (1), 163–172.

730 Davies, R. B., Harte, D., 1987. Tests for Hurst effect. *Biometrika* 74 (1),  
731 95–101.

732 Delignières, D., Fortes, M., Ninot, G., et al., 2004. The fractal dynamics of  
733 self-esteem and physical self. *Nonlinear Dynamics in Psychology and Life*  
734 *Sciences* 8, 479–510.

735 Delignieres, D., Ramdani, S., Lemoine, L., Torre, K., Fortes, M., Ninot, G.,  
736 2006. Fractal analyses for short time series: a re-assessment of classical  
737 methods. *Journal of Mathematical Psychology* 50 (6), 525–544.

738 Delignieres, D., Torre, K., 2009. Fractal dynamics of human gait: a reassess-  
739 ment of the 1996 data of Hausdorff et al. *Journal of Applied Physiology*  
740 106 (4), 1272–1279.

741 Eke, A., Herman, P., Bassingthwaite, J., Raymond, G., Percival, D., Can-  
742 non, M., Balla, I., Ikrényi, C., 2000. Physiological time series: distin-  
743 guishing fractal noises from motions. *Pflügers Archiv European Journal*  
744 *of Physiology* 439 (4), 403–415.

745 Eke, A., Herman, P., Kocsis, L., Kozak, L., 2002. Fractal characterization of  
746 complexity in temporal physiological signals. *Physiological Measurement*  
747 23 (1), R1.

748 Fougere, P. F., 1985. On the accuracy of spectrum analysis of red noise  
749 processes using maximum entropy and periodogram methods: Simula-  
750 tion studies and application to geophysical data. *Journal of Geophysical*  
751 *Research* 90 (A5), 4355–4366.

- 752 Glass, L., 2001. Synchronization and rhythmic processes in physiology. Na-  
753 ture 410 (6825), 277–284.
- 754 Glenny, R. W., Robertson, H. T., Yamashiro, S., Bassingthwaite, J. B.,  
755 1991. Applications of fractal analysis to physiology. *Journal of Applied*  
756 *Physiology* 70 (6), 2351–2367.
- 757 Goldberger, A. L., West, B. J., 1987. Fractals in physiology and medicine.  
758 *The Yale Journal of Biology and Medicine* 60 (5), 421.
- 759 Hausdorff, J. M., Lertratanakul, A., Cudkowicz, M. E., Peterson, A. L.,  
760 Kaliton, D., Goldberger, A. L., 2000. Dynamic markers of altered gait  
761 rhythm in amyotrophic lateral sclerosis. *Journal of Applied Physiology*  
762 88 (6), 2045–2053.
- 763 Hausdorff, J. M., Mitchell, S. L., Firtion, R., Peng, C. K., Cudkowicz, M. E.,  
764 Wei, J. Y., Goldberger, A. L., 1997. Altered fractal dynamics of gait:  
765 reduced stride-interval correlations with aging and Huntington’s disease.  
766 *Journal of Applied Physiology* 82 (1), 262–269.
- 767 Hausdorff, J. M., Peng, C., Ladin, Z., Wei, J. Y., Goldberger, A. L., 1995.  
768 Is walking a random walk? Evidence for long-range correlations in stride  
769 interval of human gait. *Journal of Applied Physiology* 78 (1), 349–358.
- 770 Hausdorff, J. M., Purdon, P. L., Peng, C. K., Ladin, Z., Wei, J. Y., Gold-  
771 berger, A. L., 1996. Fractal dynamics of human gait: stability of long-  
772 range correlations in stride interval fluctuations. *Journal of Applied Phys-*  
773 *iology* 80 (5), 1448–1457.
- 774 Hausdorff, J. M., Zeman, L., Peng, C. K., Goldberger, A. L., 1999. Mat-

775 uration of gait dynamics: stride-to-stride variability and its temporal or-  
776 ganization in children. *Journal of Applied Physiology* 86 (3), 1040–1047.

777 Heneghan, C., McDarby, G., 2000. Establishing the relation between de-  
778 trended fluctuation analysis and power spectral density analysis for  
779 stochastic processes. *Physical Review E* 62 (5), 6103.

780 Hu, K., Ivanov, P. C., Chen, Z., Carpena, P., Stanley, H. E., 2001. Effect  
781 of trends on detrended fluctuation analysis. *Physical Review E* 64 (1),  
782 011114.

783 Huikuri, H. V., Mäkikallio, T. H., Airaksinen, K. J., Seppänen, T., Puukka,  
784 P., Räihä, I. J., Sourander, L. B., 1998. Power-law relationship of heart  
785 rate variability as a predictor of mortality in the elderly. *Circulation*  
786 97 (20), 2031–2036.

787 Huikuri, H. V., Mäkikallio, T. H., Peng, C. K., Goldberger, A. L., Hintze, U.,  
788 Møller, M., et al., 2000. Fractal correlation properties of RR interval dy-  
789 namics and mortality in patients with depressed left ventricular function  
790 after an acute myocardial infarction. *Circulation* 101 (1), 47–53.

791 Ivanov, P. C., Amaral, L. A. N., Goldberger, A. L., Havlin, S., Rosenblum,  
792 M. G., Struzik, Z. R., Stanley, H. E., 1999. Multifractality in human  
793 heartbeat dynamics. *Nature* 399 (6735), 461–465.

794 Jones, C. L., Lonergan, G. T., Mainwaring, D. E., 1999. Wavelet packet  
795 computation of the Hurst exponent. *Journal of Physics A: Mathematical*  
796 *and General* 29 (10), 2509.

797 Kantelhardt, J. W., Koscielny-Bunde, E., Rego, H. H., Havlin, S., Bunde,  
798 A., 2001. Detecting long-range correlations with detrended fluctuation



- 799 analysis. *Physica A: Statistical Mechanics and its Applications* 295 (3),  
800 441–454.
- 801 Kantelhardt, J. W., Zschiegner, S. A., Koscielny-Bunde, E., Havlin, S.,  
802 Bunde, A., Stanley, H. E., 2002. Multifractal detrended fluctuation anal-  
803 ysis of nonstationary time series. *Physica A: Statistical Mechanics and its*  
804 *Applications* 316 (1), 87–114.
- 805 Kasdin, N. J., 1995. Discrete simulation of colored noise and stochastic  
806 processes and 1/f power law noise generation. *Proceedings of the IEEE*  
807 83 (5), 802–827.
- 808 Li, M., 2010. Fractal time series - a tutorial review. *Mathematical Problems*  
809 *in Engineering* 2010, 157264–1–26.
- 810 Li, M., Chen, S., May 20-22 2009. Fractional Gaussian noise and net-  
811 work traffic modeling. In: *Proceedings of the 8th WSEAS International*  
812 *Conference on Applied Computer and Applied Computational Science.*  
813 Hangzhou, China, pp. 34–39.
- 814 Li, M., Lim, S., 2006. A rigorous derivation of power spectrum of fractional  
815 Gaussian noise. *Fluctuation and Noise Letters* 6 (04), C33–C36.
- 816 Mallat, S. G., 1989. A theory for multiresolution signal decomposition: the  
817 wavelet representation. *IEEE Transactions on Pattern Analysis and Ma-*  
818 *chine Intelligence* 11 (7), 674–693.
- 819 Mandelbrot, B. B., 1985. Self-affine fractals and fractal dimension. *Physica*  
820 *Scripta* 32 (4), 257.
- 821 Mandelbrot, B. B., Van Ness, J. W., 1968. Fractional brownian motions,  
822 fractional noises and applications. *SIAM review* 10 (4), 422–437.

- 823 Peng, C. K., Buldyrev, S. V., Havlin, S., Simons, M., Stanley, H. E., Gold-  
824 berger, A. L., 1994. Mosaic organization of DNA nucleotides. *Physical*  
825 *Review E* 49 (2), 1685.
- 826 Peng, C. K., Havlin, S., Hausdorff, J. M., Mietus, J. E., Stanley, H. E.,  
827 Goldberger, A. L., 1995a. Fractal mechanisms and heart rate dynamics:  
828 long-range correlations and their breakdown with disease. *Journal of Elec-*  
829 *trocardiology* 28, 59–65.
- 830 Peng, C. K., Havlin, S., Stanley, H. E., Goldberger, A. L., 1995b. Quan-  
831 tification of scaling exponents and crossover phenomena in nonstationary  
832 heartbeat time series. *Chaos: An Interdisciplinary Journal of Nonlinear*  
833 *Science* 5 (1), 82–87.
- 834 Pilgram, B., Kaplan, D. T., 1998. A comparison of estimators for  $1/f$  noise.  
835 *Physica D: Nonlinear Phenomena* 114 (1), 108–122.
- 836 Schepers, H. E., Van Beek, J. H., Bassingthwaite, J. B., 1992. Four meth-  
837 ods to estimate the fractal dimension from self-affine signals (medical ap-  
838 plication). *IEEE Engineering in Medicine and Biology Magazine* 11 (2),  
839 57–64.
- 840 Sejdíć, E., Lipsitz, L. A., Aug. 2013. Necessity of noise in physiology and  
841 medicine. *Computer Methods and Programs in Biomedicine* 111 (2), 459–  
842 470.
- 843 Sharma, K., Kent-Braun, J., Majumdar, S., Huang, Y., Mynhier, M.,  
844 Weiner, M., Miller, R., 1995. Physiology of fatigue in amyotrophic lat-  
845 eral sclerosis. *Neurology* 45 (4), 733–740.

- 846 Sharma, K. R., Miller, R. G., 1996. Electrical and mechanical properties of  
847 skeletal muscle underlying increased fatigue in patients with amyotrophic  
848 lateral sclerosis. *Muscle and Nerve* 19 (11), 1391–1400.
- 849 Shlesinger, M. F., 1987. Fractal time and 1/f noise in complex systems.  
850 *Annals of the New York Academy of Sciences* 504 (1), 214–228.
- 851 Simonsen, I., Hansen, A., Nes, O. M., 1998. Determination of the Hurst  
852 exponent by use of wavelet transforms. *Physical Review E* 58 (3), 2779.
- 853 Veitch, D., Abry, P., 1999. A wavelet-based joint estimator of the parame-  
854 ters of long-range dependence. *IEEE Transactions on Information Theory*  
855 45 (3), 878–897.
- 856 Willson, K., Francis, D. P., 2003. A direct analytical demonstration of the  
857 essential equivalence of detrended fluctuation analysis and spectral anal-  
858 ysis of RR interval variability. *Physiological Measurement* 24 (1), N1.